A. Brückner-Foit, D. Munz*, and B. Trolldenier**

Micromechanical Implications of the Weakest Link Model for the Ductile–Brittle Transition Region

REFERENCE Brückner-Foit, A., Munz, D., and Trolldenier, B., **Micromechanical implications of the weakest link model for the ductile–brittle transition region**, *Defect Assessment in Components – Fundamentals and Applications*, ESIS/EGF9 (Edited by J. G. Blauel and K.-H. Schwalbe) 1991, Mechanical Engineering Publications, London, pp. 477–488.

ABSTRACT In a micromechanical interpretation of the Weakest Link model for the ductile–brittle transition region, the weak spots ahead of the crack tip which trigger fracture are described as penny-shaped cracks. The parameters of the Weibull distribution for the critical value of the J-integral at fracture are related to the statistical distribution of the crack size, and the stress field ahead of the crack tip. It is shown how this model can be used to derive an expression for the statistical distribution of the distance of the fracture origin from the crack tip. Differences between the model and experimental results obtained with CT specimens of various thicknesses can be attributed to the constraint effect, i.e. the change in the stress state with the specimen thickness.

Notation

B	Specimen thickness
B_n	Net thickness of side-grooved specimen
$F(\ )$	Probability distribution function
E	Young's modulus
J	J-integral
J_{cl}	Value of the J-integral at the onset of cleavage fracture
M	Average number of weak spots in the process zone
Q_1	Failure probability of one crack
$Q_k(u_0)$	Probability of finding one fracture origin in $(0, u_0)$ for a specimen containing k weak spots
V_{pl}	Volume of the process zone
$a_c(\vec{r})$	Critical size of a micro crack
b	Parameter of the Weibull distribution
$f(\ )$	Probability density function
k	Number of the micro cracks in one specimen
m	Exponent of the Weibull distribution
p_k	Probability of having k cracks in the process zone
r	Distance from the crack tip
u	Non-dimensional distance of the trigger point from the crack tip
w_p	Plastic work necessary for crack propagation

* Institute for Reliability and Failure Analysis, University of Karlsruhe, P.O. Box 3640, D-7500 Karlsruhe, FRG.

x Distance of the trigger point in the crack plane
x_A Distance of the trigger point from the crack tip under 0 degrees
x_B Distance of the trigger point from the crack tip under 10 degrees
y Deviation of the trigger point from the crack plane
u_{pl} Boundary of the process zone which contains all possible fracture origins
z Distance of the trigger point from the centre of the specimen
ν Poisson's ratio
γ_s Surface energy
ρ Difference of the angle by looking at the fracture surface with the scanning electronic microscope
ϕ_{pl} Angle of the boundary of the process zone
θ Angle between crack plane and the radius from the crack tip
σ_y Yield strength
$\sigma_{yy}(\vec{r})$ Component of the stress field perpendicular to the crack plane

Introduction

The Weakest Link model was introduced by Landes and Shaffer **(1)** in order to describe the scatter of the fracture toughness of ferritic steels observed in the ductile–brittle transition region (see e.g. **(2)**). Independent weak spots distributed randomly along the crack front are assumed to trigger fracture. Hence, the resistance against unstable crack extension is related to the 'strength' of the weakest spot. If the statistical distribution of the strength of the weak spots fulfils some fairly general asymptotic relations, it can be proven that the statistical distribution of the fracture strength is given by the Weibull distribution **(3)**.

A micromechanical interpretation of the Weakest Link model was given in **(4)**. A weak spot ahead of the crack front is interpreted as a crack of random crack size subjected to an external stress determined by its location in the plastic zone. Cleavage fracture of a specimen is triggered if the energy release rate of the most dangerous crack exceeds the critical energy release rate **(5)**. Using these ideas the parameter of the Weibull distribution of the fracture toughness can be related to the statistical distribution of the crack size of a weak spot and the stress field ahead of the crack tip. The same basic ideas are used in the local approach where the statistical distribution of the crack size is determined from tension tests with notched specimens **(6)**.

In most investigations in which the weakest link model is used, the effect of the multiaxiality of the stress state ahead of the crack tip is neglected. For example, the difference of the mean fracture toughness observed for specimens of different thicknesses is generally explained by the statistical size effect introduced in the original paper by Landes and Shaffer **(1)**.

In this paper the importance of the stress state for the statistical distribution of the fracture toughness will be addressed from the point of view of the

Weakest Link model and its micromechanical interpretation. In the first section it is shown how the statistical distribution of the location of the fracture origin can be used to assess the effect of the change of stress state on the parameters of the Weibull distribution. A more detailed description of the statistical model presented in this section can be found in **(7)**.

The second section contains experimental results obtained with CT-specimens of three different sizes. For each specimen these data consist of the value of J-integral at fracture as well as the coordinates of the fracture origin determined by a fractographic examination of the fracture surface. Hence, both the statistical size effect predicted by the Weakest Link model and the size effect caused by a change of the stress state can be assessed.

Statistical distribution of the location of the fracture origin

In the micromechanical interpretation of the Weakest Link model given in **(4)–(6)**, the failure probability of a cracked specimen subjected to an external loading characterised by a specific value of the applied J-integral is given by

$$P_f(J) = 1 - \exp(-MV_{pl}Q_1) \tag{1}$$

where M is the number of crack-like weak spots per unit volume, V_{pl} is the volume of the plastic zone, and Q_1 is the failure probability of one crack at an arbitrary location in the plastic zone

$$Q_1 = \frac{1}{V_{pl}} \int_{V_{pl}} \int_{a_c(\vec{r})}^{\infty} f(a)\, da\, dV_{pl} \tag{2}$$

In equation (2), $f(a)$ denotes the probability density function of the crack size of a weak spot and $a_c(\vec{r})$ is the critical crack size for a penny-shaped crack at location $\vec{r}$ in front of the crack tip

$$a_c(\vec{r}) = \frac{E(\gamma_s + w_p/2)\pi}{(1-\nu^2)2\sigma_{yy}(\vec{r})^2} \tag{3}$$

where E denotes Young's modulus, ν Poisson's ratio, $\sigma_{yy}(\vec{r})$ the value of the stress perpendicular to the crack plane and $2\gamma_s + \omega_p$ is the critical energy release rate. The extension of the plastic zone is proportional to J^2 in small-scale yielding conditions. Thus, equation (1) can be written as

$$P_f(J) = 1 - \exp\left(-\frac{J^2}{b^2}\right) \tag{4}$$

which corresponds to a Weibull distribution for the critical value J_{cl} of the J-integral with exponent $m = 2$. The location parameter b is given by

$$b = \left(M \int_0^B \int_0^{2\pi} \int_0^{u_{pl}(\theta, z)} \int_{a_c(u, \theta, z)}^{\infty} f(a)\, da\, du\, d\theta\, dz \right)^{-1} \tag{5}$$

for a specimen with crack front length B. The non-dimensional distance from the crack tip is given by

$$u = \frac{r\sigma_y}{J_{cl}} \tag{6}$$

and (r, θ) are the polar coordinates with the origin at the crack tip. If the integration domain in equation (2) is restricted to values of the non-dimensional distance u smaller than a specific value u_0, the ensuing probability $Q_1(u_0)$ with

$$Q_1(u_0) = \frac{1}{\sigma_y^2 V_{pl}/J^2} \int_0^B \int_0^{u_0} \int_0^{\theta_{pl}} \int_{a_c(u,\theta,z)}^{\infty} f(a) u \, da \, du \, d\theta \, dz \tag{7}$$

is equal to the probability that the fracture origin of a microcrack has a distance from the crack tip less than u_0. For k microcracks in the plastic zone, the quantity

$$Q_k(u_0) = k(1 - Q_1)^{k-1} Q_1(u_0) \tag{8}$$

is equal to the probability that there is one and only one fracture origin located within the distance u_0 from the crack tip and no other fracture origin elsewhere. The number of microcracks in V_{pl} is Poisson distributed random variable. Therefore, the probability of having k cracks in the plastic zone is given by

$$p_k = \frac{(MV_{pl})^k}{k!} \exp(-MV_{pl}) \tag{9}$$

Multiplying p_k with Q_k and summing over k, the number of the microcracks, and normalising the result with Q_1 yields the conditional probability that the fracture origins lies within a distance of u_0 from the crack tip for those specimen for which final cleavage fracture is triggered by one microcrack

$$F(u_0) = \frac{Q_1(u_0)}{Q_1} \tag{10}$$

Hence, the distribution $F(u)$ of the distance of the fracture origin from the crack tip depends on the stress state via the critical crack size $a_c(\bar{r})$, (see equation (3)) and equation (10) can be used to determine the importance of the constraint effect from fractographic examination of the fracture surface.

Experiments

Side-grooved CT specimens of three different thicknesses ($B = 25$ mm/$B_n = 20$ mm, $B = 12$ mm/$B_n = 9.6$ mm, $B = 6.5$ mm/$B_n = 5.2$ mm) were tested at $T = -55$°C, which corresponds to the lower part of the transition region. All specimens had a width of $W = 50$ mm and the ratio between the starting

Table 1 Material properties of the German reactor pressure vessel steel 20MnMoNi55 at test temperature $T = -55$°C

σ_y (*MPa*)	σ_u (*MPa*)	E (*MPa*)
508	688	217 000

crack length a_0 and the width W was $a_0/W = 0.6$. The material was a reactor pressure vessel steel (German designation 20MnMoNi55) whose properties are summarized in Table 1.

The J-value at final cleavage fracture was determined from the load–displacement curve using the relations given in ASTM E813-87.

The fracture surfaces of all specimens were examined in a scanning electronic microscope (SEM). Tear ridges and river patterns were used to determine the location on the fracture surface from which final cleavage fracture started. This procedure corresponds to the one described in **(9)(10)**. In all cases a unique fracture origin could be identified and an examination of both fracture surfaces lead to identical fracture origins (see Fig. 1(a)–(d)), so that there seems to be a distinct weak spot which triggers cleavage fracture in accordance with the basic assumption of the Weakest Link model. However, a crack-like disturbance of the microstructure such as an inclusion could be identified only in very few cases. This does not necessarily imply that the micromechanical interpretation of the Weakest Link model is not valid but it means that the penny-shaped microcracks introduced in the first section are idealizations of more complicated microstructural disturbances acting as weak spots.

In the fractographic examination, the coordinates of the fracture origin from the crack tip were determined (see Fig. 2). While the values of the x and z coordinates can be measured directly on the fracture surface the y coordinate can be found from the difference in the apparent location of the fracture origin determined at two different inclination angles of the specimen in the SEM. So, a projection method proposed by **(11)** was used to determine the deviation y of the fracture point from the crack plane. For this procedure a magnification has to be selected which allows the trigger point and the end of the stretched zone or the crack tip to be seen together. Then two pictures are taken under two different inclination angles (0 degrees and 10 degrees) to determine the distance y according to Fig. 3 by using the geometric relationship

$$y = \frac{x_A}{\tan \rho} - \frac{x_B}{\sin \rho} \tag{11}$$

where x_A and x_B are the measured distances and ρ the inclination difference of the angles between the two pictures.

The non-dimensional distance u (equation (6)) can thus be calculated for each specimen. Figure 4 shows the dimensionless coordinates $X = xR_{p0.2}/J_{cl}$

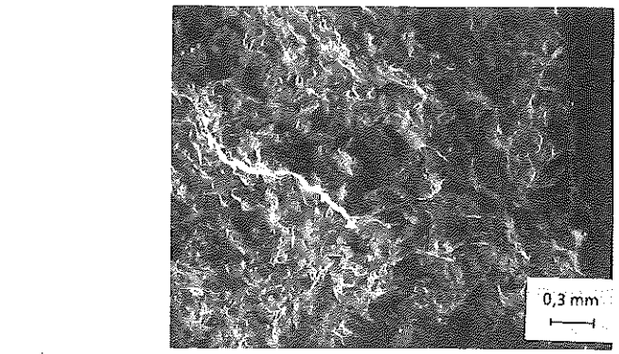

(a)

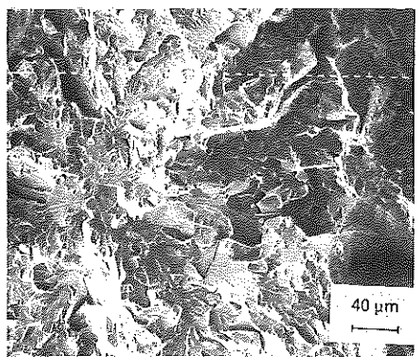

(b)

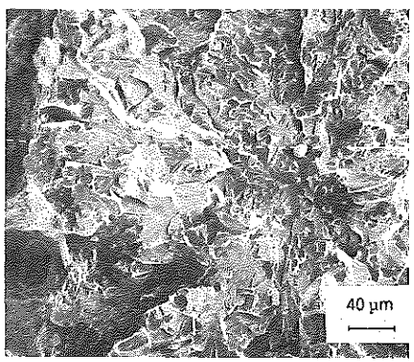

(c)

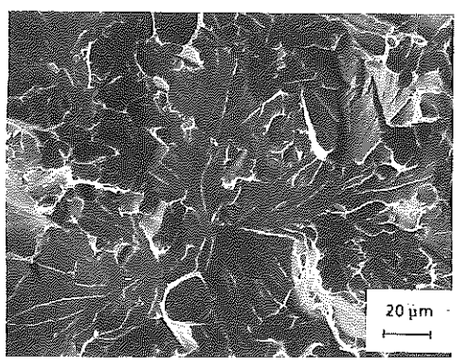

(d)

Fig 1 Identification of a fracture origin on both broken fracture surfaces

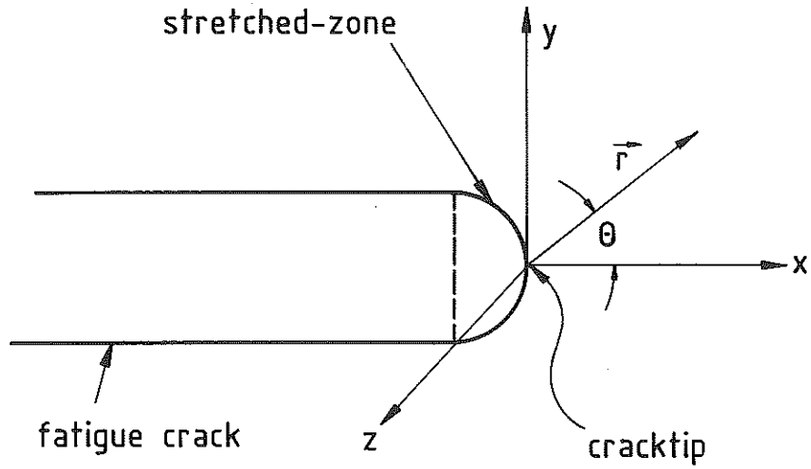

Fig 2 Coordinates at the crack tip

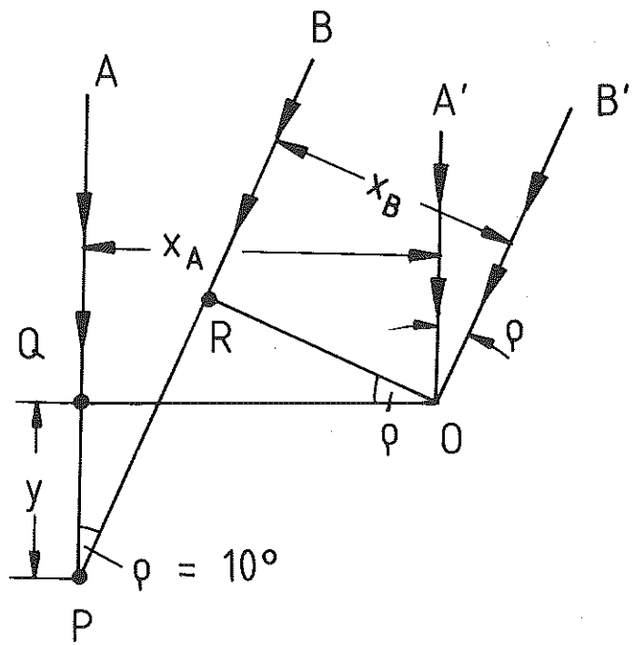

Fig 3 Location of the trigger point in the crack plane (point Q, R) under two different angles for determination of deviation *y* with equation (11)

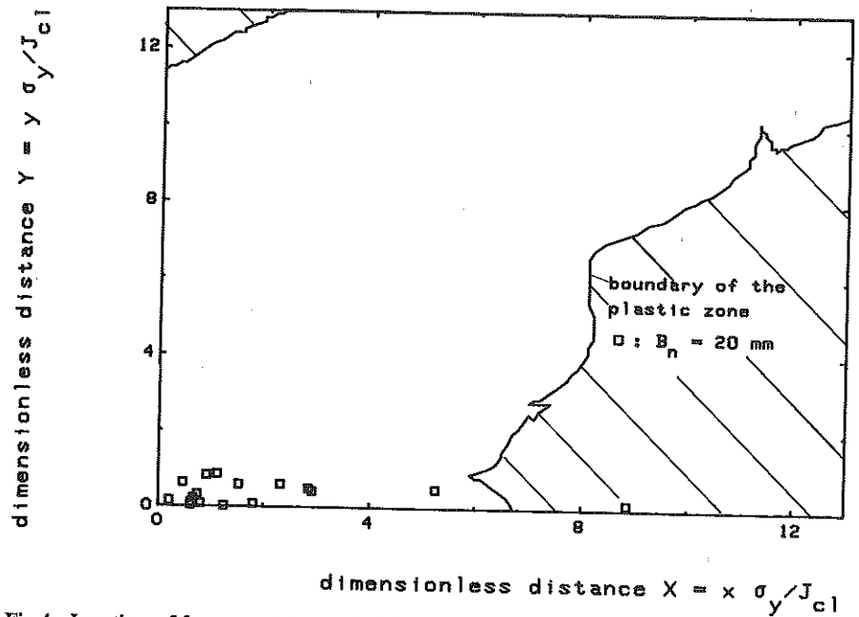

Fig 4 Locations of fracture origin ahead of the crack tip and the boundary of the plastic zone (12), $B_n = 20$ mm

and $Y = yR_{p0.2}/J_{cl}$ of the fracture origin points for the specimens with $B_n = 20$ mm. Hence the assumption is confirmed that the weak spots lie within the plastic zone. The boundary curve follows from a finite element analysis of this stress field ahead of the crack tip **(12)**.

Results

The empirical distributions of the J-integral at final cleavage fracture, J_{cl}, are shown in Fig. 5 in the form of a Weibull plot. The corresponding Weibull parameters which are summarized im Table 2 were determined using the Maximum Likelihood method (see **(13)**). The statistical uncertainty inherent in these parameters is determined by the confidence intervals which are also shown in Table 2. Seventy-six percent of the smallest specimens ($B_n = 5.2$ mm) showed a significant amount of stable crack growth. Hence, the Weibull distribution had to be truncated at the value of the J-integral, J_i, at the onset of stable crack tearing and the Maximum Likelihood evaluation procedure had to be modified in order to account for the censored sample. A more detailed description of the evaluation procedure can be found in **(14)**. Table 2 shows that the Weibull exponent m is equal to two within the limits of the statistical uncertainty given by the confidence intervals. The predictions for the location

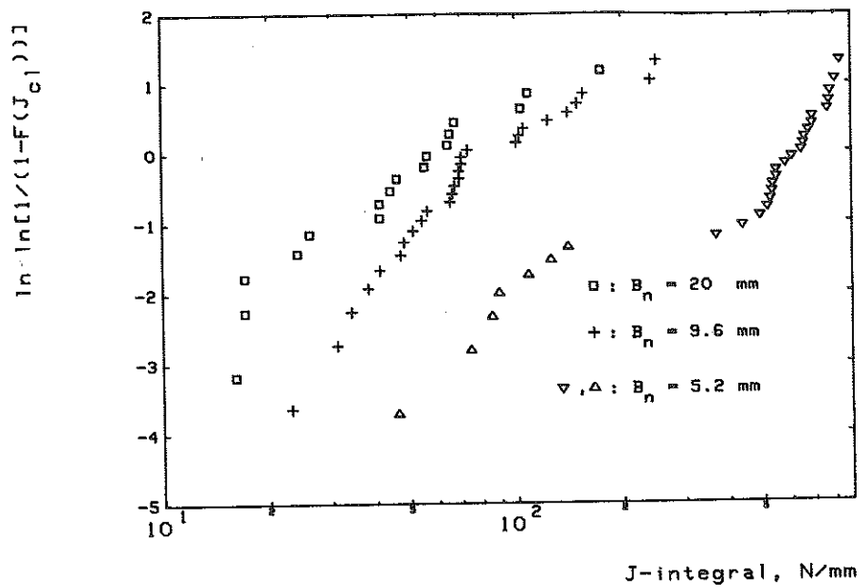

Fig 5 Complete sample of J_{cl} values obtained with CT specimen of three different thicknesses

parameter b are based on the statistical size effect

$$b_1 = b_2\left(\frac{B_2}{B_1}\right)^{1/m_2} \tag{12}$$

if two specimens of crack front length B_1 and B_2 are compared with each other (1). The predictions and the experimental results agree very well with

Table 2 Maximum likelihood estimates of the Weibull parameters and the predictions of the Weakest Link model, two-parametric distribution

	$B_n = 5.2$ mm	$B_n = 9.6$ mm	$B_n = 20$ mm
Weibull parameter m	1.18	1.67	1.57
90% confidence interval for m	(0.54, 1.67)	(1.22, 2.06)	(1.04, 2.01)
Weibull parameter b (N/mm)	657	98	64
90% confidence interval for b	(326, 1375)	(79, 112)	(47, 86)
Prediction for b from $B_n = 5.2$ mm	—	(194, 818)	(104, 439)
Prediction for b from $B_n = 9.6$ mm	(114, 176)	—	(51, 79)
Prediction for b from $B_n = 20$ mm	(111, 203)	(75, 137)	—

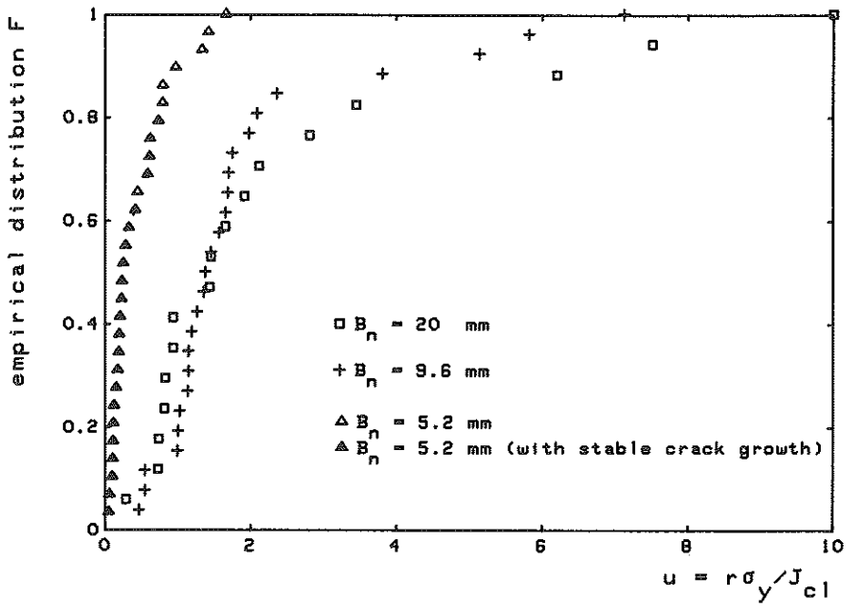

Fig 6 Empirical distribution of the non-dimensional distance u of the trigger point from the crack tip

each other for the thickness ($B_n = 20$ mm) and the medium size ($B_n = 9.6$ mm) specimens, but the value of b obtained for the thin specimens ($B_n = 5.2$ mm) exceeds the value predicted from the other two test series.

The empirical distributions (Fig. 6) of the non-dimensional distance u of the fracture origin from the crack tip shows that the deviations obtained for the J_{cl}-values of the smallest specimens can be attributed to a constraint effect. While the empirical distributions of u determined for $B_n = 20$ mm and $B_n = 9.6$ mm show no statistically significant deviation from each other, the function $F(u)$ seems to be shifted to lower values of u for $B_n = 5.2$ mm. In the case of the specimens with $B_n = 5.2$ mm, those specimens showing stable crack growth prior to cleavage fracture are included in the empirical distribution of the non-dimensional distance u. This procedure is justified if the stress field ahead of the crack tip remains virtually unchanged during stable crack growth. This assumption is of course questionable and is subject of further investigations. This difference of $F(u)$ for the different specimen thicknesses can be explained qualitatively by the fact that the degree of the multiaxiality and hence the equivalent stress determining the critical crack size (see equation (3)) is reduced in the thinner specimens so that the weak spots have to lie closer to the crack tip in order to trigger the cleavage fracture. The same conclusion is reached if the variation of J along the crack front is considered (see **(15)**) instead of an equivalent stress.

Conclusions

The distribution of the value of the J-integral at cleavage fracture, J_{cl}, and the results of an extensive fractographic investigation of the fracture surfaces confirm the basic assumptions and the predictions of the Weakest Link model and its micromechanical interpretation.

- The coordinates of the weak spots lie within the boundary of the plastic zone. This is also in agreement with the local approach where the parameters of the statistical distribution of the weak spots are evaluated using the yielded zones of notched tensile specimens **(6)**.
- The Weibull exponent of the J_{cl} distribution m agrees very well with the theoretical value $m = 2$.
- The statistical size effect as it is predicted by the Weakest Link model is confirmed by the results obtained with 1CT- and 1/2CT-specimens. The location parameter b of the Weibull distribution exceeds the predicted value for the smallest specimen.

The deviation between the Weakest Link model and the empirical distributions of J_{cl} can be attributed to the change in the stress state for the specimens of different sizes. This hypothesis is supported by the empirical distributions of the non-dimensional distance u of the fracture origin from the crack tip.

References

(1) LANDES, J. D. and SHAFFER, D. H. (1980) Statistical characterisation of fracture in the transition region, *ASTM STP 700*, pp. 368–382.
(2) IWADATE, T., TANAKA, Y., ONO, S. and WATANABE, J. (1983) An analysis of elastic–plastic–fracture–toughness behaviour for J_{Ic} measurement in the transition region, *ASTM STP 803*, pp. II/531–II/561.
(3) GUMBEL, E. (1958) *Statistics of Extremes*, Columbia University Press, New York.
(4) WALLIN, K., SAARIO, T. and TÖRRONEN, K. (1984) Statistical model for carbide induced brittle fracture in steel, *Met. Sci.*, **18**, 337–347.
(5) CURRY, D. A. and KNOTT, J. F. (1976) The relationship between fracture toughness and microstructure in the cleavage fracture of mild steel, *Met. Sci.*, 1–6.
(6) MUDRY, F. (1987) A local approach to cleavage fracture, *Nucl. Engng Des.*, **105**, 65–76.
(7) BRÜCKNER-FOIT, A., EHL, W., MUNZ, D. and TROLLDENIER, B. (1990) The size effect and microstructural implications of the weakest—link–model, *Fatigue Fracture Engng Mater. Structures*, **13**, 185–200.
(8) SLATCHER, S. (1986) A probabilistic model for lower-shelf fracture toughness – theory and application, *Fatigue Fracture Engng Mater. Structures*, 275–289.
(9) EHL, W. (1987) *Bruchmechanische, statististiche und fraktographische Untersuchungen am Stahl 20 Mn Mo Ni 55 im duktil–spröden Übergangsbereich*, Dissertation, Universität Karlsruhe.
(10) ROSENFIELD, A. R., SHETTY, D. K. and SKIDMORE, A. J. (1983) Fractographic observations of cleavage initiation in the ductile–brittle transition region of a reactor–pressure–vessel steel, Report of Battelle Laboratories, Columbus, OH.
(11) OHTSUKA, N. (1987) Fractographic discussion on fracture toughness test specimen in the transition temperature region, *Trans 9th Int. Conf. Structl Mech. in Reactor Technology (SMiRT9)* (Edited by F. Wittman), **G**, A. Balkema Publications, pp. 77–82.
(12) MEMHARD, D. and OKKEWITZ, A. private communication.
(13) THOMAN, D. R., BAIN, C. J. and ANTLE, C. E. (1969) Inferences on the parameters of the Weibull–distribution, *Technometrics*, **11**, 445–460.

(14) BRÜCKNER-FOIT, A., MÜNZ, D. and TROLLDENIER, B. (1990) Internal Report.
(15) KAWANO, S., TADA, M., YAJIMA, H. and NAGAI, K. (1986) Thickness effect on brittle fracture toughness of weld metal of high tensile strength steel, IIW Doc. No. X-1121-86, International Welding Institute.